Hyperfine interactions in the 13 K ferromagnet $Eu_2Si_5N_8$

Henning A. Höppe[a], Henning Trill[b], Bernd D. Mosel[b], Hellmut Eckert[b], Gunter Kotzyba[a], Rainer Pöttgen[a], Wolfgang Schnick[a,*]

[a]*Department Chemie, Ludwig-Maximilians-Universität, München, Butenandtstraße 5-13 (Haus D), D-81377 Munich, Germany*
[b]*Institut für Physikalische Chemie, Universität Münster, Schloßplatz 4/7, D-48149 Münster, Germany*

1. Introduction

Polymeric non-metallic nitrides are of considerable interest for the development of inorganic materials with potential high-performance applications [1,2]. In contrast to the well known oxosilicates, nitridosilicates contain SiN_4 tetrahedra which can be linked via common vertices resulting in $N^{[2]}$, $N^{[3]}$, and even $N^{[4]}$ connections of two, three, or four silicon atoms, respectively, [1,3]. Accordingly, the nitridosilicates show a more versatile connectivity pattern as compared to oxosilicates leading to a significant extension of conventional silicate chemistry.

In recent years, several new alkaline earth and rare earth metal-based nitridosilicates like $LnSi_3N_5$ (Ln = La, Ce, Pr, Nd) [3–5], $Ln_3Si_6N_{11}$ (Ln = Ce, Pr) [6,7], BaEu$(Ba_{0.5}Eu_{0.5})YbSi_6N_{11}$ [8], $MYbSi_4N_7$ (M = Sr, Ba, Eu) [9–11]) or $Eu_2Si_5N_8$ [11] have been synthesized. The structures of these nitridosilicates are built up from highly condensed Si–N networks with predominant covalent bonding leading to outstanding chemical, thermal and mechanical stability.

Although the structures of these materials are well known, only little information is available on the physical properties. Our recent studies of the optical properties of the europium doped phases $Ba_{2-x}Eu_xSi_5N_8$ [12] revealed long lasting luminescence, thermoluminescence and two-photon-excitation. Very broad absorption and emission bands have been observed which are typical for Eu^{2+} and which are broadened due to the presence of two overlaying crystallographic Eu^{2+} sites. Additionally, these bands show an exceptional strong red shift as compared with common Eu^{2+} containing optical materials [13–15]. This behaviour has been ascribed to the different nitrogen coordination of the Eu^{2+} ions [12].

We have now extended the physical property investigations with respect to the magnetic behaviour and ^{151}Eu Mössbauer spectroscopy. Details about the magnetic hyperfine interactions of the europium atoms in $Eu_2Si_5N_8$ are reported herein.

2. Experimental

2.1. Synthesis and X-ray powder data

The synthesis of $Eu_2Si_5N_8$ was performed in a radio-frequency furnace (type IG 10/200 Hy, frequency: 200 kHz, electrical output: 0–12 kW, Hüttinger, Freiburg) according

* Corresponding author. Tel.: +49-89-2180-7436; fax: +49-89-2180-7440.
E-mail address: wsc@cup.uni-muenchen.de (W. Schnick).

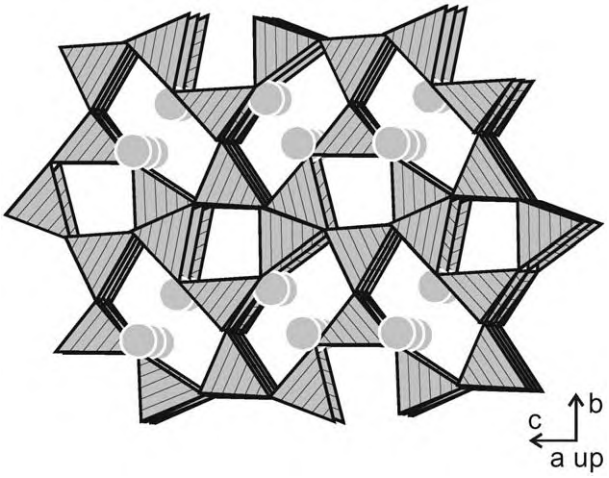

Fig. 1. Perspective view of the $Eu_2Si_5N_8$ structure approximately along the *a* axis. The europium atoms fill channels within the three-dimensional network of corner-sharing SiN_4 tetrahedra.

to Eq. (1).

$$2Eu + 5Si(NH)_2 \rightarrow Eu_2Si_5N_8 + 5H_2 + N_2 \quad (1)$$

Under argon a mixture of 129 mg (2.22 mmol) silicon diimide [16] and 125 mg (0.823 mmol) europium metal (ABCR, 99.9%) was transferred into a tungsten crucible. The latter was then heated under nitrogen to 1070 K within 5 min in the water-cooled quartz-reactor of the radiofrequency furnace [17]. After 25 min, the crucible was heated to 1820 K within 12 h and held at this temperature for another 6 h. Subsequent quenching to room temperature within 30 min yielded single-phase $Eu_2Si_5N_8$. The excess europium metal evaporated off the reaction mixture and condensed at the inner surface of the water-cooled quartz-reactor. $Eu_2Si_5N_8$ was obtained as a coarsely crystalline, bright red powder. More details about the experimental setup are given in Refs. [17,18].

The purity of our sample was checked by X-ray powder diffraction (Stoe Stadi P) using Cu $K\alpha_1$ radiation. The pattern could completely be indexed on the basis of a primitive orthorhombic cell and the refined lattice parameters ($a = 570.85(7)$ pm, $b = 681.42(8)$ pm, $c = 933.42(16)$ pm, space group $Pmn2_1$) were in excellent agreement with the previously published data [11].

2.2. Physical property measurements

The magnetic susceptibilities of a polycrystalline, powdered sample of $Eu_2Si_5N_8$ were determined with a MPMS *XL* SQUID magnetometer (Quantum Design) in the temperature range 4.2–300 K with magnetic flux densities up to 5 T. A quantity of 8.534 mg was enclosed in a small silica tube and fixed at the sample holder rod. The sample was then cooled to 4.2 K in zero magnetic field and slowly heated to room temperature in an applied external field.

The 21.53 keV transition of ^{151}Eu with an activity of 130 MBq (2% of the total activity of a $^{151}Sm:EuF_3$ source) was used for the Mössbauer spectroscopic experiments. The measurements were performed with a commercial helium bath cryostat. The temperature of the absorber could be varied from 4.2 to 300 K and was measured with a metallic resistance thermometer with a precision better than ±0.5 K. The source was kept at room temperature. The material for the Mössbauer spectroscopic investigation was the same as for the susceptibility measurements. The sample was diluted with sugar and placed within a thin-walled PVC container at a thickness corresponding to about 10 mg Eu/cm^2.

3. Results and discussion

3.1. Crystal chemistry

$Eu_2Si_5N_8$ crystallizes with the previously described $Ba_2Si_5N_8$ type structure [18] with the non-centrosymmetric space group $Pmn2_1$. The crystallographically determined absence of an inversion centre has been proven by observation of two-photon absorption [12]. As outlined in Fig. 1, the crystal structure is based on a network of corner sharing SiN_4 tetrahedra. In this network, half of the nitrogen atoms connect two ($N^{[2]}$), and the other ones three silicon atoms ($N^{[3]}$). The Eu^{2+} cations occupy two different sites within the channels running along the *a* axis. These channels are formed by Si_6N_6 rings (Fig. 1). The nitrogen coordination of the Eu1 (CN 10) and Eu2 (CN 8 + 2) atoms is presented in Fig. 2. For a more detailed discussion of the crystal chemistry, we refer to the previous work [11,17]. Chemical bonding in isostructural $Sr_2Si_5N_8$ was investigated recently by first-principles electronic band structure calculations [19]. These investigations revealed a large band gap (>4 eV) as expected for these transparent compounds.

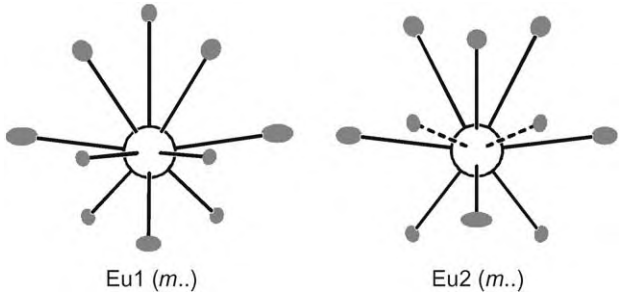

Fig. 2. Nitrogen coordination of the two crystallographically different europium atoms in $Eu_2Si_5N_8$. The site symmetries are indicated. The displacement ellipsoids of the nitrogen atoms represent 90% probability.

3.2. Magnetic properties

In Fig. 3 we present the temperature dependence of the inverse magnetic susceptibility of $Eu_2Si_5N_8$ measured at magnetic flux densities of 0.1 and 3 T. Above 50 K we observe Curie–Weiss behaviour, $\chi = C/(T - \Theta)$ with an experimental magnetic moment of $7.67(5)\mu_B$/Eu, close to the free ion value of $7.94\mu_B$ for Eu^{2+}. Thus the formula $Eu_2Si_5N_8$ is consistent with formal oxidation states Eu^{2+}, Si^{4+}, and N^{3-}. The paramagnetic Curie temperature (Weiss constant) of $\Theta = 18(1)$ K was determined by linear extrapolation of the $1/\chi$ vs T data to $1/\chi = 0$. In the 3 T measurement we observe no *bump* around 70 K where EuO orders ferromagnetically [20–22], indicating pure $Eu_2Si_5N_8$. Small EuO impurities are sometimes observed for europium intermetallics [23,24].

At low temperature ferromagnetic ordering of the europium magnetic moments is detected (Fig. 4). The Curie temperature of $T_C = 13.0(5)$ K was determined from the derivative $d\chi/dT$ of a kink-point measurement (insert of Fig. 4) at a magnetic flux density of 0.002 T. The observed difference between the susceptibility curves taken upon cooling in zero (ZFC, zero field cooling) and non-zero (FC, field cooling) magnetic field may be attributed to domain effects. The field cooling measurement yields considerably higher values of the magnetization in the ordered region, because it corresponds to probing of the response to the magnetic field of a nearly single domain sample.

The magnetization behaviour at 100 and 4.5 K is shown in Fig. 5. At 100 K we observe a linear increase of the magnetization as expected for a paramagnetic material. A steep increase occurs at 4.5 K. Already around 2 T the magnetization tends towards saturation, reaching a saturation magnetic moment of $7.0(1)\mu_B$/Eu at 5 T. This value is consistent with the maximal possible value of $7\mu_B$/Eu according to $g \times S$ [25], indicating full parallel spin alignment at low temperatures. According to the very small hysteresis and the almost negligible coercivity and remanence $Eu_2Si_5N_8$ might be classified as a soft ferromagnet.

Based on the magnetic data, one cannot distinguish two different europium sites. Below the Curie temperature of 13 K we observe a cooperative parallel alignment of all europium magnetic moments.

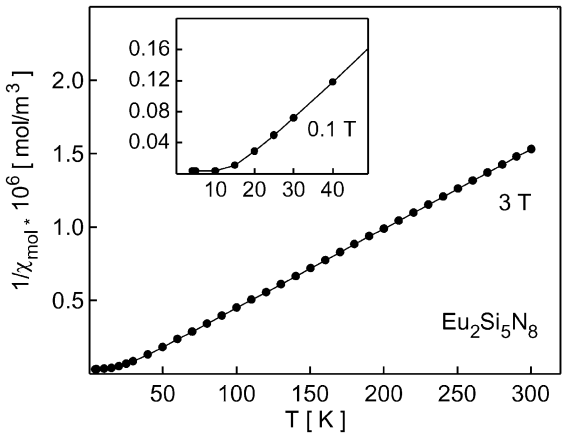

Fig. 3. Temperature dependence of the inverse magnetic susceptibility of $Eu_2Si_5N_8$ measured at 3 T. The low-temperature behaviour at 0.1 T is shown in the insert.

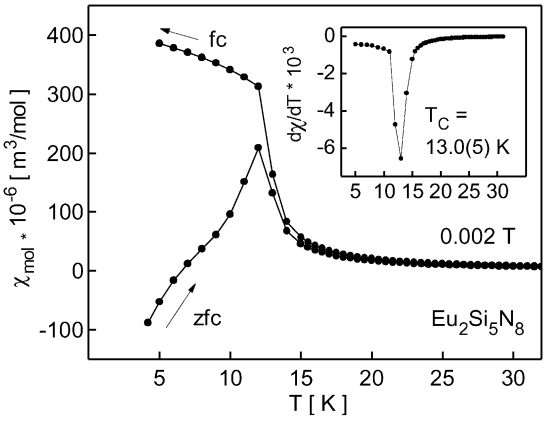

Fig. 4. Low-temperature susceptibility of $Eu_2Si_5N_8$ measured at an external field strength at 0.002 T in the zero-field-cooling (ZFC) and field-cooling (FC) modus. The insert shows the derivative $d\chi/dT$ which has a sharp peak at $T_C = 13.0(5)$ K.

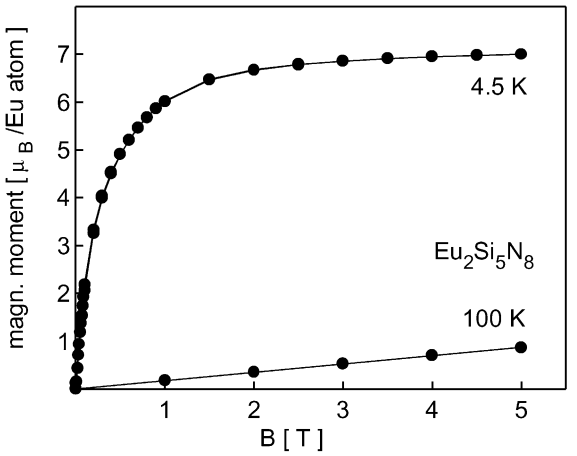

Fig. 5. Magnetization vs external field strength of $Eu_2Si_5N_8$ measured at 4.5 and 100 K.

3.3. *^{151}Eu Mössbauer spectroscopy*

Temperature dependent ^{151}Eu Mössbauer spectra of $Eu_2Si_5N_8$ are presented in Fig. 6. Transmission integral fits were obtained using the Levenberg–Marquard algorithm, resulting in the parameters isomer shift, nuclear electric quadrupolar splitting, asymmetry parameter, line width, and internal magnetic flux density at the europium nuclei. The refined parameters are listed in Table 1. Although the crystal structure has two crystallographically different europium sites in a 1:1 ratio, these sites are not resolvable in the spectrum. Rather, a single set of parameters was found to provide a satisfactory fit to the experimental data. Above the Curie temperature, the spectrum is dominated by a large quadrupolar splitting, which reflects the low site symmetry (*m*…) of both europium positions. The magnitude of the splitting is comparable to that observed for several intermetallic europium transition metal (T) indides and stannides EuTIn and EuTSn [26,27], where the europium atoms have the same site symmetry.

The close similarity of both europium sites was rationalized with electric field gradient (EFG) calculations, assuming that the electron density distribution arising from the five direct Eu–N bonds in the first coordination sphere produces the dominant term in the local EFG experienced by the ^{151}Eu nuclei. Table 2 summarizes all of the Eu–N internuclear distances within a 400 pm sphere around the two central europium sites. The corresponding charges on nitrogen as calculated by the Brown/Shannon method are also included. A sizeable valence contribution to the ^{151}Eu EFG is expected only from the nitrogen atoms N1, N2, and N3, which are engaged in only two Si–N bonds. For each europium site, the valence term was estimated on the basis

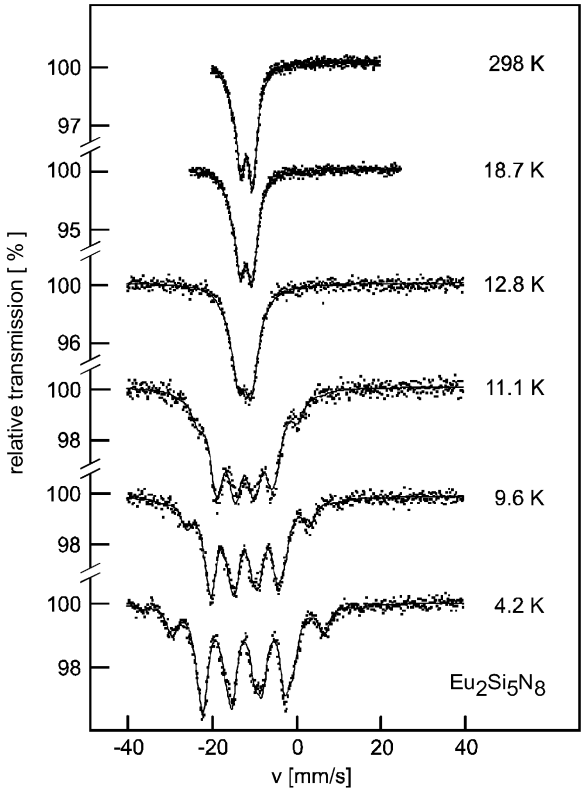

Fig. 6. Experimental and simulated ^{151}Eu Mössbauer spectra of $Eu_2Si_5N_8$ at different temperatures.

Table 1
^{151}Eu Mössbauer fitting parameters for $Eu_2Si_5N_8$ as a function of temperature. The numbers in parentheses give the statistical errors in the last digit. Values without parentheses were kept fixed by the fitting program (for details see text). δ, isomer shift with respect to EuF_3; Γ, experimental line width; ΔE_Q, electric quadrupole interaction; B, static magnetic flux density

T (K)	δ (mm/s)	Γ (mm/s)	ΔE_Q (mm/s)	Asymmetry	B (T)
298	−11.82(5)	2.3(1)	16.8(2)	0.67(7)	0
18.7	−11.88(5)	2.5(1)	16.6(2)	0.73(9)	0
12.8	−11.9(1)	3.4(3)	16.8(2)	0.8(2)	0
11.1	−11.8(1)	3.4(3)	−3.10(6)	0	16.4(3)
9.6	−11.78(7)	2.9(2)	−3.10(4)	0	20.1(2)
4.2	−11.80(7)	2.5(1)	−3.36(3)	0	24.9(2)

of a point charge model calculation, using the atomic positions, Eu–N distances and local charges listed for those nitrogen atoms (marked by asterisks in Table 2). Nitrogen atoms engaged in three Si–N bonds were excluded from the EFG calculation, even if the corresponding Eu–N distances appear to be similar. Any contributions arising from point charges generated by other non-Eu-bonded atoms in the structure were also assumed negligible compared to the valence contribution. Using a Sternheimer antishielding parameter of 70 (estimated from Lucken's data on related rare earth nuclei) [28] the calculated EFG principal values and asymmetry parameters are: Eu1 : $V_{zz} = 1.18 \times 10^{22}$ V/m^2; $\eta = 0.95$; Eu2 : $V_{zz} = 1.27 \times 10^{22}$ V/m^2; $\eta = 0.47$. We find these values to be in quite good agreement with the experimental value of 1.05×10^{22} V/m^2, $\eta = 0.7$ as determined from the single site Mössbauer lineshape fit.

The calculations confirm the close similarity in the local bonding environments of Eu1 and Eu2. Because of the large natural linewidth of the ^{151}Eu Mössbauer transition, the 10% difference in the nuclear electric quadrupolar coupling constants predicted in the calculation cannot be resolved in the spectra.

At temperatures below 13 K characteristic line broadening

Table 2
Eu–N distances (in pm) and nitrogen atomic charges of all nitrogen atoms within a 400 pm sphere of Eu1 or Eu2. All those distances included in the field gradient calculations are marked by asterisks. The closest distances around the N atoms are listed on the right side of the table. Note that N1, N2, and N3 possess only two Si–N bonds. Thus, Eu–N bonding involving these nitrogen atoms is expected to produce a valence contribution to the europium electric field gradient

Eu site	Distance	N site	N charge	N site	Distance	Cation site
Eu1	252.9*	N1	−1.53	N6	175.9	Si4
	272.4*	N3	−1.62		175.9	Si4
	272.4*	N3	−1.62		176.8	Si1
	289.3*	N2	−1.56	N5	173.5	Si3
	289.3*	N2	−1.56		175.2	Si4
	297.5	N4	−1.69		175.2	Si4
	297.5	N4	−1.69	N4	176.5	Si3
	315.8	N3	−1.62		176.9	Si1
	315.8	N3	−1.62		178.3	Si4
	324.6	N6	−1.63	N3	168.2	Si4
	380.9	N6	−1.63		171.9	Si2
					258.9	Eu2
Eu2	255.4*	N2	−1.56		272.4	Eu1
	258.9*	N3	−1.62	N2	166.8	Si3
	258.9*	N3	−1.62		171.8	Si2
	289.0*	N1	−1.53		255.4	Eu2
	289.0*	N1	−1.53		289.3	Eu1
	290.2	N5	−1.53		289.3	Eu1
	323.5	N4	−1.69	N1	167.2	Si1
	323.5	N4	−1.69		171.0	Si2
	341.7	N3	−1.62		252.9	Eu1
	341.7	N3	−1.62		289.0	Eu2
	394.3	N6	−1.63		289.0	Eu2

and the development of a magnetic hyperfine splitting indicates the onset of magnetic ordering, in agreement with the magnetic susceptibility data discussed earlier. This effect is associated with a dramatic reduction in the magnitude of the EFG parameter used to optimise the least squares fit to the data, suggesting that the angle defining the orientation of the EFG principal axis with respect to the magnetic hyperfine field direction is close to the magic angle. A similar situation has been previously observed in EuPdIn [26].

At 11.1 K, slightly below the Curie temperature, a large magnetic hyperfine field of 16.4(3) T is detected at the nuclei. Since we cannot distinguish between the two Eu sites, this value must be considered as an average over both positions. Down to 4.2 K the flux density at the europium nuclei increases to 24.9(2) T, as is typically observed for magnetically ordered Eu(II) compounds [23,29].

4. Conclusions

In the present study, we investigated the magnetic hyperfine interactions in the nitridosilicate $Eu_2Si_5N_8$. Magnetic susceptibility and ^{151}Eu Mössbauer spectroscopic experiments revealed purely divalent europium in $Eu_2Si_5N_8$, however, it was not possible to distinguish the two crystallographically independent europium sites by the latter techniques. We observe a superposition of both europium sites. Ferromagnetic ordering of the europium magnetic moments is observed at $T_C = 13$ K. At 4.2 K the saturation magnetization is $7.0(1)\mu_B$/Eu and the hyperfine field at the europium nuclei is 24.9(2) T.

Acknowledgements

This work was financially supported by the Fonds der Chemischen Industrie and especially by the Deutsche Forschungsgemeinschaft (Gottfried-Wilhelm-Leibniz-Programm).

References

[1] W. Schnick, Solid-state chemistry with nonmetal nitrides, Angew. Chem. Int. Ed. Engl. 32 (1993) 806–818.
[2] H.-P. Baldus, M. Jansen, Novel high-performance ceramics—amorphous inorganic networks from molecular precursors, Angew. Chem. Int. Ed. Engl. 36 (1997) 328–343.
[3] M. Woike, W. Jeitschko, Preparation and crystal structure of the nitridosilicates $Ln_3Si_6N_{11}$ (Ln = La, Ce, Pr, Nd, Sm) and $LnSi_3N_5$ (Ln = Ce, Pr, Nd), Inorg. Chem. 34 (1995) 5105–5108.
[4] Z. Inoue, M. Mitomo, N. Il, A crystallographic study of a new compound of lanthanum silicon nitride $LaSi_3N_5$, J. Mater. Sci. 15 (1980) 2915–2920.
[5] M. Woike, W. Jeitschko, Crystal structure of cerium silicon nitride (1/3/5), $CeSi_3N_5$, Z. Kristallogr. 211 (1996) 813.
[6] T. Schlieper, W. Schnick, High-temperature synthesis crystal structure, and magnetic properties of $Ce_3[Si_6N_{11}]$, Z. Anorg. Allg. Chem. 621 (1995) 1535–1538.
[7] T. Schlieper, W. Schnick, Crystal structure of tripraseodymiumhexasiliconundecanitride, $Pr_3Si_6N_{11}$, Z. Kristallogr. 211 (1996) 254.
[8] H. Huppertz, W. Schnick, Synthesis and crystal structure of $BaEu(Ba_{0.5}Eu_{0.5})YbSi_6N_{11}$, Z. Anorg. Allg. Chem. 624 (1998) 371–374.
[9] H. Huppertz, W. Schnick, Synthesis crystal structure, and properties of the nitridosilicates $SrYbSi_4N_7$ and $BaYbSi_4N_7$, Z. Anorg. Allg. Chem. 623 (1997) 212–217.
[10] H. Huppertz, W. Schnick, $BaYbSi_4N_7$—unexpected structural possibilities in nitridosilicates, Angew. Chem. Int. Ed. Engl. 35 (1996) 1983–1984.
[11] H. Huppertz, W. Schnick, $Eu_2Si_5N_8$ and $EuYbSi_4N_7$—the first nitridosilicates with a divalent rare earth, Acta Crystallogr. C53 (1997) 1751–1753.
[12] H.A. Höppe, H. Lutz, P. Morys, W. Schnick, A. Seilmeier, Luminescence in Eu^{2+} doped $Ba_2Si_5N_8$: fluorescence thermoluminescence, and upconversion, J. Phys. Chem. Solids 61 (2000) 2001–2006.
[13] E. Pedrero, J. Hernandez, C. Flores, A. Garcia-Borquez, J.O. Tocho, M. Villagrán-Muniz, J. García Solé, H. Murrieta, Analysis of the optical behaviour of Eu^{2+} ions in CsCl crystals, Phys. Status Solidi B 203 (1997) 591–598.
[14] B. Moine, C. Pedrini, B. Courtois, Photoionization and luminescences in BaF_2:Eu^{2+}, J. Lumin. 50 (1991) 31–38.
[15] S.H.M. Poort, G. Blasse, The influence of the host lattice on the luminescence of divalent europium, J. Lumin. 72 (1997) 247–249.
[16] H. Lange, G. Wötting, G. Winter, Silicon nitride—from powder to ceramic materials, Angew. Chem. Int. Ed. Engl. 30 (1991) 1579–1597.
[17] W. Schnick, H. Huppertz, R. Lauterbach, High-temperature syntheses of novel nitrido- and oxonitridosilicates and sialons using RF furnaces, J. Mater. Chem. 9 (1999) 289–296.
[18] T. Schlieper, W. Milius, W. Schnick, High temperature syntheses and crystal structures of $Sr_2Si_5N_8$ and $Ba_2Si_5N_8$, Z. Anorg. Allg. Chem. 621 (1995) 1380–1384.
[19] C.M. Fang, H.T. Hintzen, G. de With, R.A. de Groot, Electronic structure of the alkaline-earth silicon nitrides $M_2Si_5N_8$ (M = Ca and Sr) obtained from first-principles calculations and optical reflectance spectra, J. Phys.: Condens. Matter 13 (2001) 67–76.
[20] B.T. Matthias, R.M. Bozorth, J.H. Van Vleck, Ferromagnetic interaction in EuO, Phys. Rev. Lett. 5 (1961) 160–161.
[21] D.B. McWhan, P.C. Souers, G. Jura, Magnetic and structural properties of europium metal and europium monoxide at high pressure, Phys. Rev. 143 (1966) 385–389.
[22] B. Stroka, J. Wosnitza, E. Scheer, H.v. Löhneysen, W. Park, K. Fischer, Specific heat of europium strontium oxide ($Eu_xSr_{1-x}O$) near the ferromagnetic phase transition, Z. Phys. B: Condens. Matter 89 (1992) 39–43.
[23] R. Pöttgen, D. Johrendt, Equiatomic intermetallic europium compounds: syntheses, crystal chemistry, chemical bonding, and physical properties, Chem. Mater. 11 (2000) 875–897.
[24] R. Mishra, R. Pöttgen, R.-D. Hoffmann, D. Kaczorowski, H. Piotrowski, P. Mayer, C. Rosenhahn, B.D. Mosel, Ternary rare earth (RE) gold compounds REAuCd and RE_2Au_2Cd, Z. Anorg. Allg. Chem. 627 (2001) 1283–1291.

[25] H. Lueken, Magnetochemie, Teubner, Stuttgart, 1999.
[26] R. Müllmann, B.D. Mosel, H. Eckert, G. Kotzyba, R. Pöttgen, A ^{151}Eu Mössbauer spectroscopic and magnetic susceptibility investigation of the intermetallic compounds EuTIn (T = Zn, Pd, Pt, Au), J. Solid State Chem. 137 (1998) 174–180.
[27] R. Müllmann, U. Ernet, B.D. Mosel, H. Eckert, R.K. Kremer, R.-D. Hoffmann, R. Pöttgen, A ^{119}Sn and ^{151}Eu Mössbauer spectroscopic, magnetic susceptibility, and electrical conductivity investigation of the stannides EuTSn (T = Cu, Pd, Ag, Pt), J. Mater. Chem. 11 (2001) 1133–1140.
[28] E.A.C. Lucken, Nuclear quadrupole coupling constants, Academic Press, London, 1969.
[29] F. Grandjean, G.J. Long, Mössbauer spectroscopy applied to inorganic chemistry, vol. 3, Plenum Press, New York, 1989.